
INVESTIGATION OF THE EFFECT OF PROCESS PARAMETERS IN CO₂ LASER CUTTING OF PMMA MATERIAL BY RESPONSE SURFACE METHOD

Emre KURT *^{ID}
Umut Efe KARAÇAY *^{ID}
Mümin TUTAR **^{ID}

Received: 17.12.2022; revised: 13.07.2023; accepted: 14.07.2023

Abstract: Recently, the studies on lightweighting have gained significant importance due to requirements such as energy efficiency and sustainability. Polymer materials are a group of materials that are frequently used for this purpose. This study investigated the effects of laser power, cutting speed and focal point on the kerf width, which are the most effective process parameters in laser cutting of Polymethylmethacrylate, a low-cost polymer material, using Response Surface Methodology and ANOVA. The results obtained from the data analysis show that the kerf width is seriously affected by the focal point depth as well as the speed and power.

Keywords: Laser cutting, PMMA, Response Surface Method

Pmma Malzemesinin Co₂ Lazer Kesiminde İşlem Parametrelerinin Etkisinin Yanıt Yüzey Metodu İle Araştırılması

Öz: Son zamanlarda enerji verimliliği ve sürdürülebilirlik gibi gereksinimler nedeniyle hafifletme çalışmaları büyük önem kazanmıştır. Polimer malzemeler bu amaçla sıklıkla kullanılan bir malzeme grubudur. Bu çalışmada, düşük maliyetli bir polimer olan Polymethylmethacrylate malzemesinin lazer kesiminde en etkili işlem parametreleri olan lazer gücü, kesme hızı ve odak noktasının kerf genişliği üzerindeki etkileri Yanıt Yüzey Metodu ve ANOVA kullanılarak incelenmiştir. Veri analizinden elde edilen sonuçlar, çentik genişliğinin hız ve gücün yanı sıra odak noktası derinliğinden ciddi şekilde etkilendiğini göstermektedir.

Anahtar Kelimeler: Lazer kesim, PMMA, Yanıt Yüzey Metodu

1. INTRODUCTION

With the development of technology, the strength/weight ratio of the material has gained great importance in all kinds of designs in recent years, depending on the useful load. The use of lightweight materials such as thermoplastic polymers is increasing to reduce the weight of the

* Milli Savunma Üniversitesi Hava Astsubay Meslek Yüksekokulu, Fatih Mh, Ege Cd. No:3, 35410 Gaziemir / İZMİR

** Bursa Uludağ Üniversitesi Yenişehir İbrahim Orhan Meslek Yüksekokulu, İznik Yolu Üzeri 3.Km, 16900 Yenişehir / BURSA

Correspondence Author: Emre KURT (ekurt@msu.edu.tr)

material without reducing its strength and also to allow recycling. Thermoplastics are usually presented in granular form, softening and melting when heated and become fluid. Thanks to this feature, the material's physical properties are recycled without much deterioration. Polymethylmethacrylate (PMMA) is a low-cost thermoplastic polymer with properties such as high visual transparency, low density and high absorbency (Cavdar ve Tanrisever 2013, Kamal et al. 2020, Monsores et al. 2019, Vakili-Tahami et al. 2019). PMMA, like other polymers, can be used in different applications, generally in the automotive and aerospace industries (Becker ve Locascio 2002, Bora 2014, Falco et al., Georgopoulou et al. 2020, Piana et al. 2019).

Changing and developing technology has also changed material processing methods. Laser cutting technologies used to cut polymer materials provide many advantages over traditional cutting techniques (Khoshaim et al. 2021). CO₂ laser cutting is a method used to cut both metal-based materials and non-metallic materials. As a working principle; It consists of the movement of the focused laser beam perpendicular to the plane of the surface to be cut. The heat generated by the focused beam creates a hole in the material and the material is cut by the moving beam (Aniszewska et al. 2020, Masoud et al. 2020, Yuce 2019). PMMA is very suitable for CO₂ laser cutting as it has a high wavelength absorbance of 95%. CO₂ laser cutting is used to cut highly complex shapes, reducing shape cutting limitations and increasing corner strengths by reducing stress on material edges. Because PMMA has high wavelength absorption, it produces high cut quality and minimal microcracks in the material (Dudala et al. 2020, Khamar ve Prakash 2020, Prakash ve Kumar 2015).

In the literature review, it has been observed that more research is needed on the optimization of laser cutting parameters of PMMA materials laser cut with CO₂ laser beam. In this study, the effects of laser power, cutting speed and focal point, which are the most effective process parameters in laser cutting with CO₂ laser beam, on the kerf width (Kw) were investigated with the help of Response Surface Methodology (RSM). In this context, the singular and interactive effects of the process parameters were determined by analysis of variance (ANOVA). With the desirability function approach, optimum process parameters were determined to minimize the kerf width.

This study investigated the effects of cutting speed, laser power and focal point position, which are CO₂ laser cutting parameters, on the kerf width of PMMA material . It is aimed to determine the effect of parameters on kerf width values using Response Surface Methodology (RSM). The general trend of the effect of these variable parameters on the cutting surface properties was observed. ANOVA was used to analyze and understand the kerf width on the cut surface of different parameters.

2. EXPERIMENTAL DETAILS

2.1. Materials and Method

The physical, mechanical and thermal properties of the used PMMA material were given in Table 1. The dimensions of the produced PMMA specimens were 90 mm in length x 25 mm in width and 3 mm in thickness.

Table 1. Physical, mechanical and thermal properties of PMMA

Density (kg/m ³)	Thermal conductivity (W m ⁻¹ K ⁻¹)	Heat capacity (kJ kg ⁻¹ K ⁻¹)	Flammability UL94	Thermal expansion coeff. (K ⁻¹)	Melting temp. (K)	Water Absorption (%)	Ultimate strength (MPa)
1180	0.193	1.42	HB	7x10 ⁻⁵	433	0.3	72.4

Unilaser branded LT-1080 CCD model 1000 mm x 800 mm single head laser cutting device was used for this study (Fig. 1). This device has peak power of 120W, 0°C – 45°C working environment, servo and step motor motion system, 2200W air suction system, 5000 Chiller cooling technology, water cooling system and honeycomb table type.

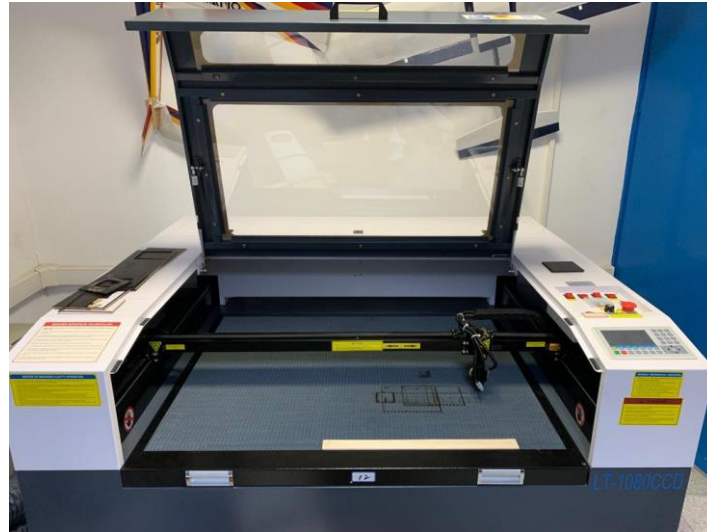


Figure 1:
Laser cutting device

The laser cutting direction and specimen geometry made in RDWorks are transferred to the laser cutting device via USB (Fig. 2). The cutting process was finished 2 mm after the end of the specimens. The aim is to remove the effect of slowing down the insert on the kerf width at the end of the process.

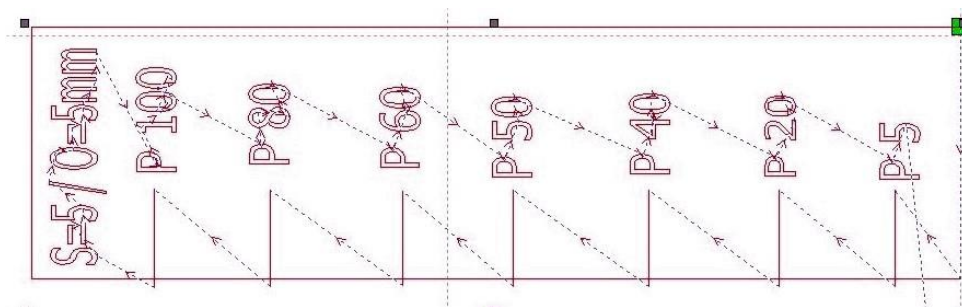


Figure 2:
Laser cutting direction and specimen geometry

Factors affecting the kerf width of PMMA material cut with CO₂ laser cutting, cutting speed, laser power and focal point position.

As shown in Figure 3, various parameters affecting the kerf width were tested with preliminary tests. The cutting parameters giving minimum and maximum heat input were determined by preliminary experiments.

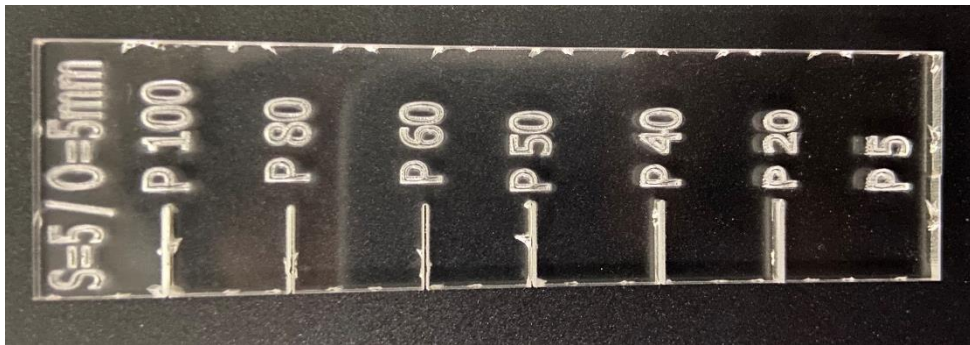


Figure 3:
Preliminary test specimen

Laser power: The rated power of the laser cutting device is 100 W. Preliminary experiments were carried out to determine the parameter levels. 60%, 80% and 100% values of maximum power were selected, respectively.

Focal Point Position: To examine the effect of the focal point on the kerf width, values of -4mm and +4mm were chosen from the optimum level.

Cutting Speed: Cutting speed was selected as 10 mm/s, 15 mm/s and 20 mm/s.

RSM is an assembling of mathematical and statistical models used to examine the effect of input parameters affecting a product or process on optimization and output parameters (Ahmed et al. 2016, Alahmari et al. 2016, Sarıkaya ve Yılmaz 2018, Venkatesan et al. 2016). RSM, provides optimization using less experimental design. RSM, defines interactive relationships between process parameters (Borse ve Kadam 2018, Ghosal ve Manna 2013). Levels of process parameters given in Table 2.

Table 2. Levels of Process Parameters

Cutting Speed (S) (mm/s)	Focal Point (F) (mm)	Laser Power (P) (%)
10	1	60
15	5	80
20	9	100

In this study, Celestron Handheld Digital Microscope Pro was used for measuring kerf width values. This device has a 20x to 200x magnification range, 5MP sensor size, 1.75 μ m pixel size and CMOS Sensor in lieu of eyepiece.

First, the cross-sectional images of samples were captured and then, kerf width values were measured using WebPlotDigitizer.

3. RESULT AND DISCUSSION

Fig. 3. shows an example of microscope images taken for measuring the kerf width values. As shown in micrographs, kerf width on the upper and lower surface of the samples are different. Since the kerf widths on the upper surface are larger in all samples, this value, which is the largest kerf width, was taken as the response.

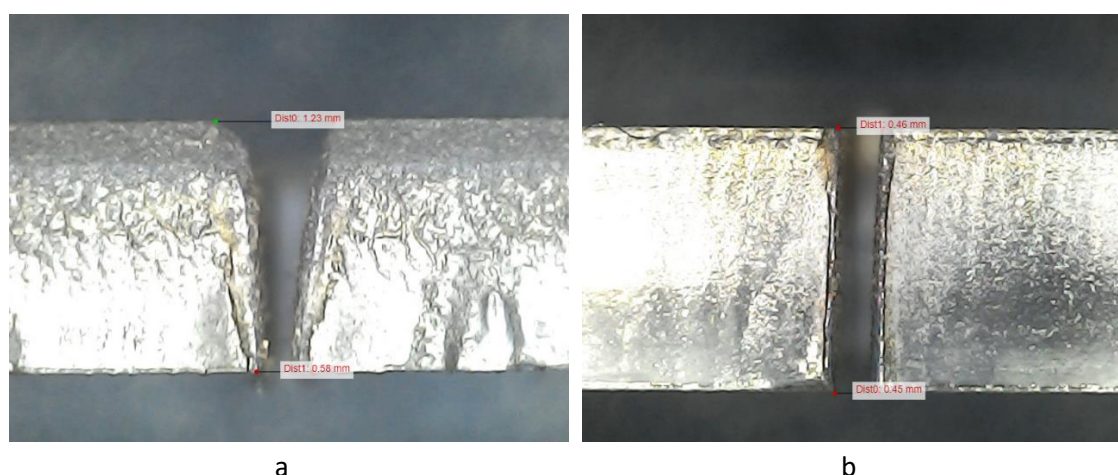


Figure 4:
Kerf widths of specimens

The kerf width of the specimen shown in Figure 4a (S10F1P60) was measured as 1.23 mm, and the kerf width of the specimen given in 4b (S10F9P80) was measured as 0.46 mm. All measured kerf width values are tabulated in Table 3 with nomenclature of samples and relevant parameter levels.

Experiments were performed as per design of experimental to analyze the impact of the focal point upon kerf width. This methodology helps study the complex relationships between input parameters. The design of experiment prepared by using Minitab 17 is shown in Table 3.

Table 3. Experimental design and measured values

Test No	Nomenclature	Laser Power (%)	Cutting Speed (mm/s)	Focal Point (mm)	Kerf Width (mm)
1	S10F5P60	60	10	5	0.50
2	S10F5P100	100	10	5	0.68
3	S20F5P60	60	20	5	0.50
4	S20F5P100	100	20	5	0.52
5	S15F1P60	60	15	1	1.23
6	S15F1P100	100	15	1	1.25
7	S15F9P60	60	15	9	0.50
8	S15F9P100	100	15	9	0.53
9	S10F1P80	80	10	1	1.38
10	S20F1P80	80	20	1	0.83
11	S10F9P80	80	10	9	0.46
12	S20F9P80	80	20	9	0.45
13	S15F5P80	80	15	5	0.50
14	S15F5P80	80	15	5	0.50
15	S15F5P80	80	15	5	0.50

The impacts of the input parameters (laser power, cutting speed, focal point) on Kerf Width were obtained by applying ANOVA to data obtained during experimentation. ANOVA results are shown in Table 3. The confidence level of ANOVA for kerf width was taken as 95%. This model is statistically acceptable and determines the significant input parameters and their effect on kerf width. The R² value of the model is 98.27%. This shows that there are significant relations between input parameters and obtained kerf width values. Source, degrees of freedom (DF), adjusted sum of squares (Adj SS), adjusted mean squares (Adj MS), F-values and percentage contribution (% Contribution) of each parameter and various interactions are as shown in Table 4. The contribution of individual parameter and their interactions indicates the significance of each parameter. The regression equation of kerf width including linear, square and nonlinear terms is shown in second-order polynomial equation (1), representing the relationship between kerf width and the other parameters. The ANOVA results and their coded coefficients for the equation (1) were shown in Table 5.

$$\text{Kerf Width (mm)} = 2.554 - 0.0221 A + 0.0087 B - 0.3795 C + 0.000184 A * A - 0.00095 B * B + 0.01898 C * C - 0.000400 A * B + 0.000031 A * C + 0.00675 B * C \quad (1)$$

where A is Laser power (%), B is Cutting speed (mm/s) and C is Focal point (mm).

Table 4. ANOVA for RSM

Source	DF	Adj SS	Adj MS	F-Value	Contribution
Model	9	1.45695	0.161883	31.59	98.27%
Linear	3	1.01792	0.339308	66.21	68.66%
Laser Power (%)	1	0.00781	0.007812	1.52	0.53%
Cutting Speed (mm/s)	1	0.06480	0.064800	12.64	4.37%
Focal Point (mm)	1	0.94531	0.945312	184.45	63.76%
Square	3	0.35970	0.119899	23.40	24.26%
Laser Power (%)*Laser Power (%)	1	0.02008	0.020083	3.92	0.73%
Cutting Speed (mm/s)* Cutting Speed (mm/s)	1	0.00208	0.002083	0.41	0.56%
Focal Point (mm)*Focal Point (mm)	1	0.34067	0.340667	66.47	22.98%
2-Way Interaction	3	0.07933	0.026442	5.16	5.35%
Laser Power (%)*Cutting Speed (mm/s)	1	0.00640	0.006400	1.25	0.43%
Laser Power (%)*Focal Point (mm)	1	0.00003	0.000025	0.00	0.00%
Cutting Speed (mm/s)*Focal Point (mm)	1	0.07290	0.072900	14.22	4.92%
Error	5	0.02563	0.005125		1.73%
Lack-of-Fit	3	0.02563	0.008542	*	1.73%
Pure Error	2	0.00000	0.000000		0.00%
Total	14				100.00%

Table 5. The results of the Analysis of Variance for the Eq. (1).

Term	Coef	SE Coef	T-Value	P-Value	VIF
Constant	0.5000	0.0413	12.10	0.000	
Power (%)	0.0313	0.0253	1.23	0.272	1.00
Speed (mm/s)	-0.0900	0.0253	-3.56	0.016	1.00
Focal Point (mm)	-0.3437	0.0253	-13.58	0.000	1.00
Power (%)*Power (%)	0.0738	0.0373	1.98	0.105	1.01
Speed (mm/s)*Speed (mm/s)	-0.0238	0.0373	-0.64	0.552	1.01
Focal Point (mm)*Focal Point (mm)	0.3037	0.0373	8.15	0.000	1.01
Power (%)*Speed (mm/s)	-0.0400	0.0358	-1.12	0.315	1.00
Power (%)*Focal Point (mm)	0.0025	0.0358	0.07	0.947	1.00
Speed (mm/s)*Focal Point (mm)	0.1350	0.0358	3.77	0.013	1.00

The normal probability plot of the residuals of kerf width is as shown in Fig. 5. The marked dots in the graph show the obtained values. The closeness of these points to the linear line indicates that the regression model well fitted with the observed data and the errors were distributed consistently.

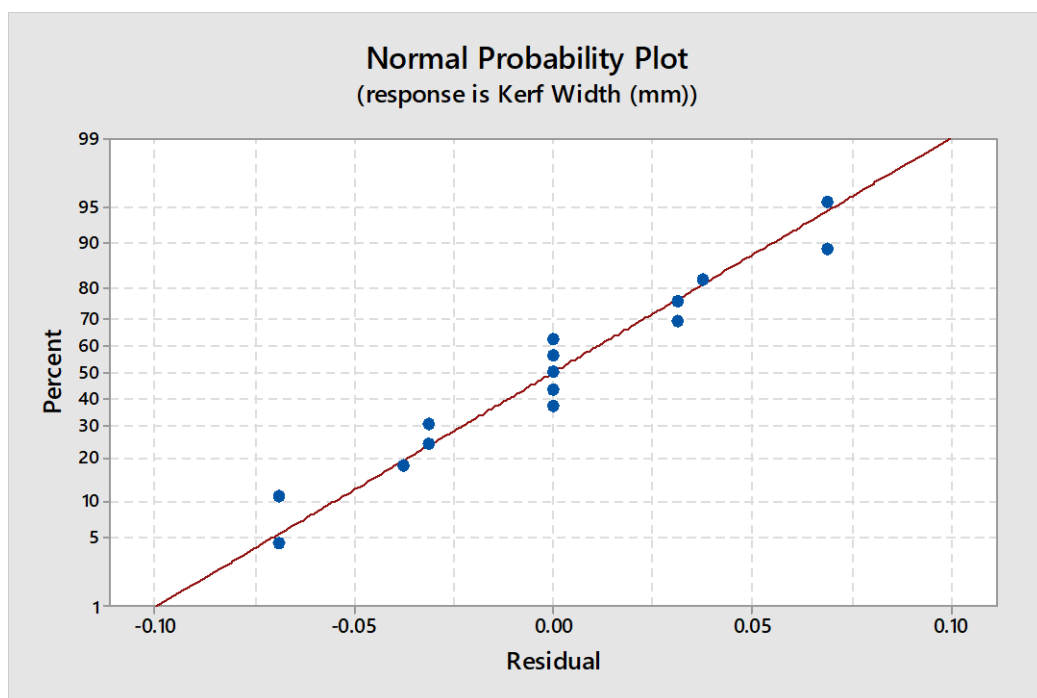


Figure 5:
Normal probability plot for Kw

The main effect plot for kerf width is shown in Fig. 6. The increase in cutting speed decreases the kerf width. The kerf width also increases with increasing laser power. This effect is attributed to increase of heat input. Both increase in laser power and decrease in cutting speed increases the heat input as shown in Eq 2 (Son ve Lee 2020). E_{volume} is volume energy, P_{laser} is the laser power [W], V_s is the cutting speed [mm/min], and A is the spot area of the laser beam [mm].

$$E_{volume} = \frac{P_{laser}}{V_s \times A} (J/m^3) \quad (2)$$

Kerf width initially decreases by an increase in focal point and further increases by an increase in focal point. The heat input localization is determined by focal point parameter. So, kerf width is seriously affected by focus depth as seen in Fig. 6.

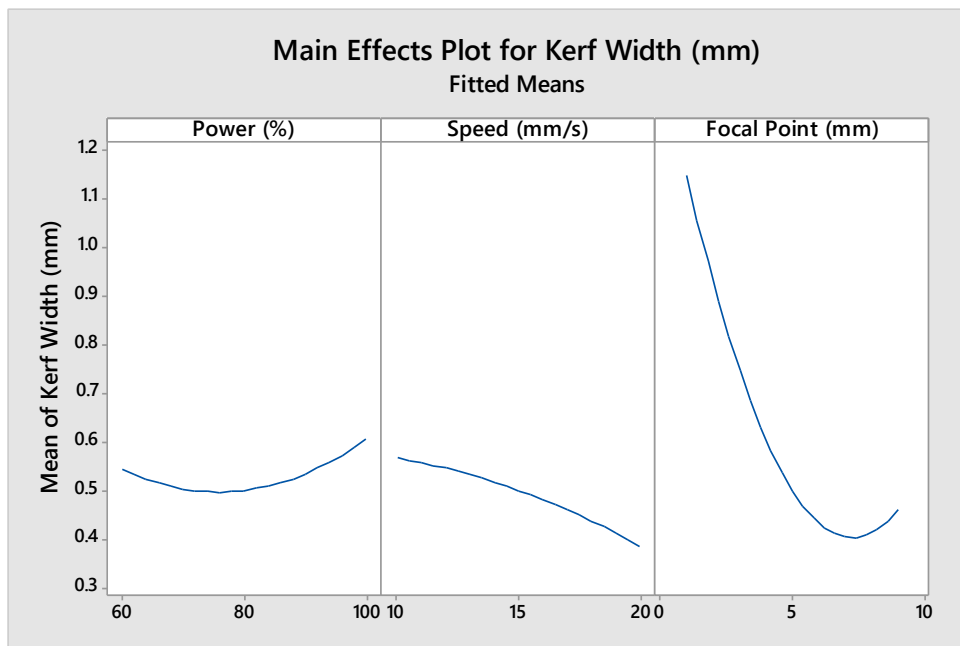


Figure 6:
Main effect plot for Kw

The main effect plot shows the effect of only one parameter, while the interaction plot shows how the response is affected due to the interaction of the two parameters. In Fig. 7, interaction plot is given. For example, upper right plot (Focal Point * Power) shows us how kerf width value changes while focal point increasing. In this plot, different curves with different color and line style are attributed to levels of Power parameter. Similar to the results in Figure 6, the interaction plot also showed the significant effect of Focal point on kerf width.

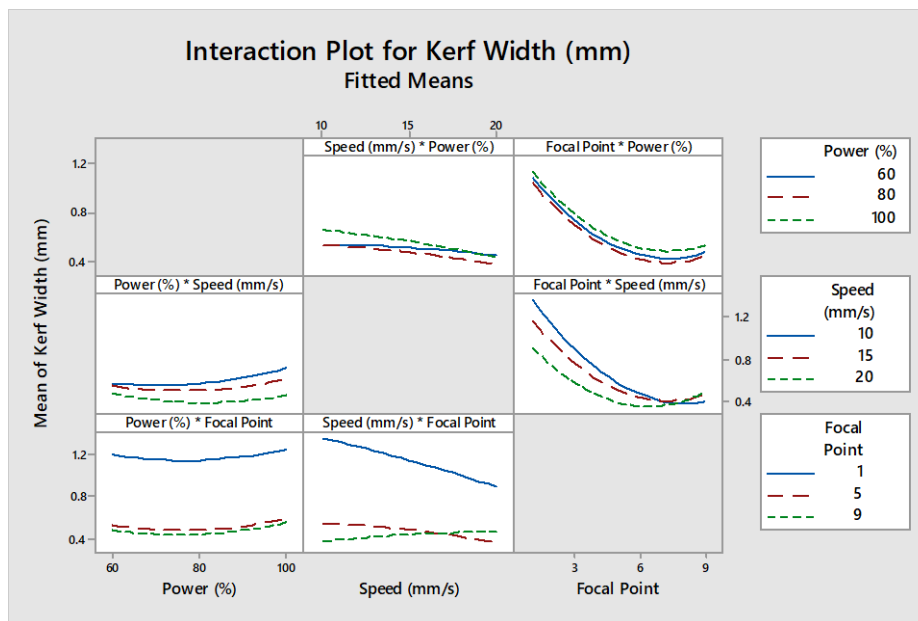


Figure 7:
Interaction plot for Kw

As shown in Fig. 8, when the focal point is hold values at 5 mm, the kerf width increased as the laser power was increased and the cutting speed decreased. When laser power constant cutting speed is decreased, kerf width increased.

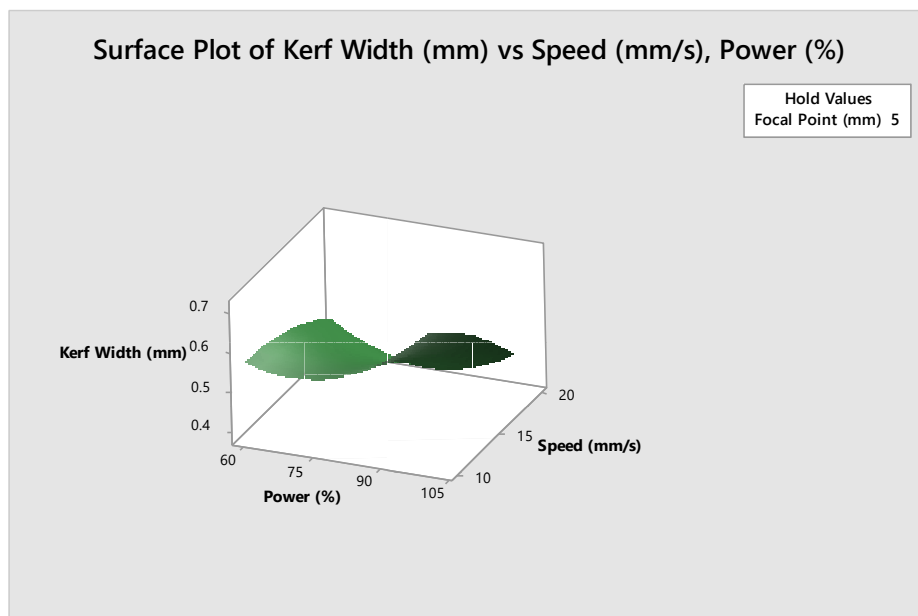


Figure 8:
Surface plot for Kw vs cutting speed, power

As shown in Fig. 9, when the cutting speed is hold values at 15 mm/s, when the focal point is hold values at 5mm, the kerf width increased as the laser power was increased and the focal point decreased. When focal point kept constant, kerf width increases almost linearly with laser power.

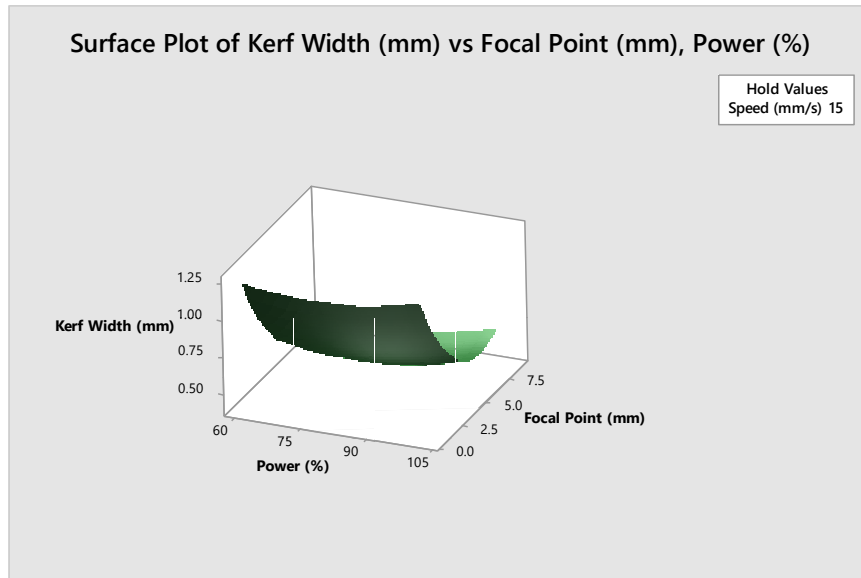


Figure 9:
Surface plot for Kw vs focal point, power

As shown in Fig. 10, when the laser power is hold values at 80%, it showed a graph similar to Figure 8. The kerf width increases as the focal point and cutting speed decrease.

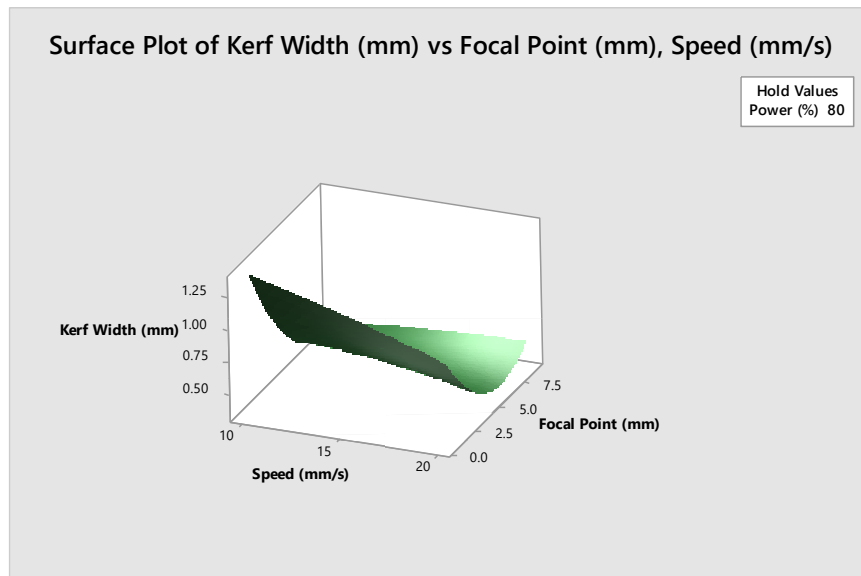


Figure 10:
Surface plot for Kw vs focal point, cutting speed

As shown in Fig. 11, when the laser power is 80%, speed is 15 mm/s and focal point hold values at 5 mm, from the speed* power graph, decreasing speed and increasing power will increase the kerf width. From focal point*power graph, the kerf width increases with decreasing focus and increasing power. From focal point*speed graph, the kerf width increases with decreasing focus and speed. In addition, the power remains constant in the focus* power graph and the focal point decreases, and the speed remains constant in the focus* speed graph and the focal point decreases, causing the kerf width to increase.

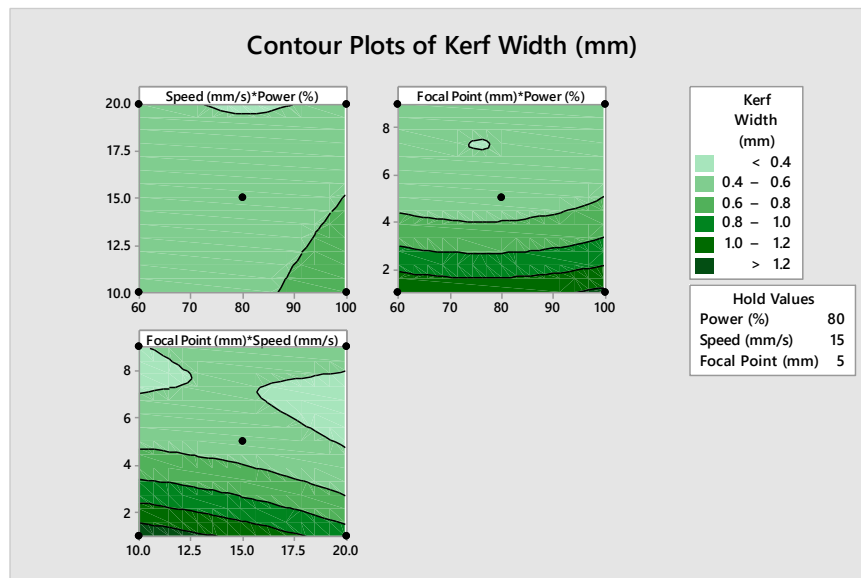


Figure 11:
Contour plot for Kw

The desirability function approach, which is a mostly used method for optimizing response surfaces, was used to determine the optimum process parameters minimizing kerf width. Figure 12 shows individual desirability plot for minimizing the kerf width. As can be seen in the figure, the parameter set giving the minimum kerf width of 0.36 mm was obtained as %70.10, 10mm/s and 8.19mm for laser power, cutting speed and focal point, respectively.

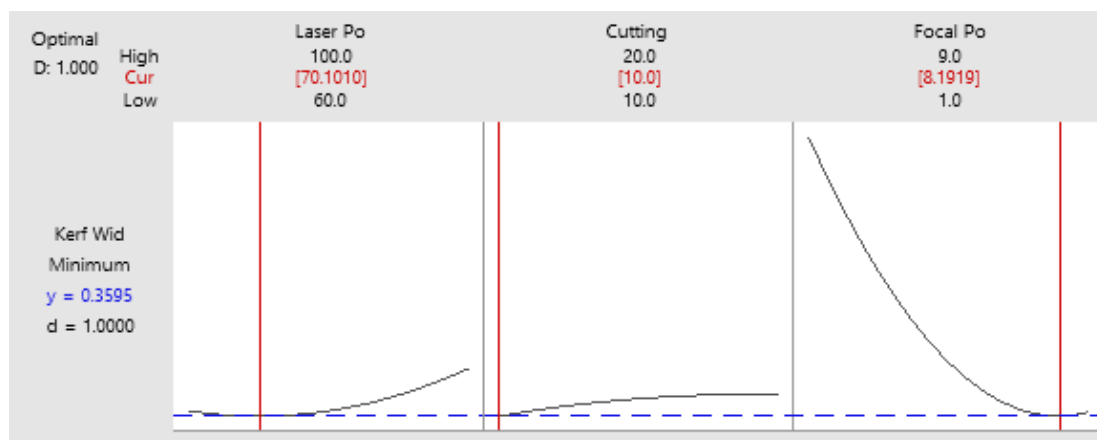


Figure 12:
Individual desirability plot

4. CONCLUSIONS

In this investigation, the effects of laser cutting parameters on kerf width values were evaluated. PMMA sheets were cut in accordance with the parameter sets obtained by the Box Behnken response surface method. The resulting kerf widths were imaged and measured using microscope. The obtained main conclusions can be summarized as follows:

- Confidence level of ANOVA for kerf width was found as 95%. This model determines the significant input parameters and their effect on kerf width. This the R² value of the model is 98.27% and is statistically acceptable.
- The results obtained from the data analysis show that the kerf width is seriously affected by the focal point depth as well as the speed and power.
- It has been found that when focal point kept constant, kerf width increases almost linearly with the laser power and laser power is the second significantly parameter.
- It has been found that when the laser power hold values at 80%, the kerf width increases with decreasing focus and increasing power, when speed hold values at 15 mm/s, the kerf width increases with decreasing focus and increasing power and when focal point hold values at 5 mm, decreasing speed and increasing power will increase the kerf width.

CONFLICT OF INTEREST

Authors approve that to the best of their knowledge, there is not any conflict of interest or common interest with an institution/organization or a person that may affect the review process of the paper.

AUTHOR CONTRIBUTION

Dr. Mümin TUTAR determining the concept and design process of the research management, data analysis and interpretation of results, Emre KURT research management, data collection and analysis, Umut Efe KARACAY data collection and analysis.

REFERENCES

1. Ahmed, N., Alahmari, A. M., Darwish, S., and Naveed, M. (2016). Laser beam micro-milling of nickel alloy: dimensional variations and RSM optimization of laser parameters. *Applied Physics A*, 122, 1-16. doi.org/10.1007/s00339-016-0553-2
2. Alahmari, A. M., Darwish, S., and Ahmed, N. (2016). Laser beam micro-milling (LBMM) of selected aerospace alloys. *The International Journal of Advanced Manufacturing Technology*, 86, 2411-2431. doi.org/10.1007/s00170-015-8318-1
3. Aniszewska, M., Maciak, A., Zychowicz, W., Zowczak, W., Mühlke, T., Christoph, B., ... and Sujecki, S. (2020). Infrared laser application to wood cutting. *Materials*, 13(22), 5222. doi.org/10.3390/ma13225222
4. Becker, H., and Locascio, L. E. (2002). Polymer microfluidic devices. *Talanta*, 56(2), 267-287. doi.org/10.1016/S0039-9140(01)00594-X
5. Bora, M. Ö. (2014). The influence of heat treatment on scratch behavior of polymethylmethacrylate (PMMA). *Tribology International*, 78, 75-83. doi.org/10.1016/j.triboint.2014.04.030

6. Borse, S. C., and Kadam, M. S. (2018). Experimental Study in micromilling of Inconel 718 by fiber laser machining. *Procedia Manufacturing*, 20, 213-218. doi.org/10.1016/j.promfg.2018.02.031
7. Cavdar, K., and Tanrısever, T. (2013). Farklı Malzemelerin Lazerle Kesilmesi. *Uludağ Üniversitesi Mühendislik Fakültesi Dergisi*, 18(2), 79-99. doi.org/10.17482/uujfe.99888
8. Dudala, S., Rao, L. T., Dubey, S. K., Javed, A., and Goel, S. (2020). Experimental characterization to fabricate CO2 laser ablated PMMA microchannel with homogeneous surface. *Materials Today: Proceedings*, 28, 804-807. doi.org/10.1016/j.matpr.2019.12.302
9. Falco, M., Simari, C., Ferrara, C., Nair, J. R., Meligrana, G., Bella, F., ... and Gerbaldi, C. (2019). Understanding the effect of UV-induced cross-linking on the physicochemical properties of highly performing PEO/LiTFSI-based polymer electrolytes. *Langmuir*, 35(25), 8210-8219. doi.org/10.1021/acs.langmuir.9b00041.
10. Georgopoulou, A., Kummerlöwe, C., and Clemens, F. (2020). Effect of the elastomer matrix on thermoplastic elastomer-based strain sensor fiber composites. *Sensors*, 20(8), 2399. doi.org/10.3390/s20082399
11. Ghosal, A., and Manna, A. (2013). Response surface method based optimization of ytterbium fiber laser parameter during machining of Al/Al2O3-MMC. *Optics & Laser Technology*, 46, 67-76. doi.org/10.1016/j.optlastec.2012.04.030
12. Kamal, A., Elsheikh, A. H., and Showaib, E. (2020, November). Pre-Cracking techniques of polymeric materials: an overview. In *IOP Conference Series: Materials Science and Engineering* (Vol. 973, No. 1, p. 012028). IOP Publishing. doi.org/10.1088/1757-899X/973/1/012028
13. Khamar, P., and Prakash, S. (2020). Investigation of dimensional accuracy in CO2 laser cutting of PMMA. *Materials Today: Proceedings*, 28, 2381-2386. doi.org/10.1016/J.MATPR.2020.04.711
14. Khoshaim, A. B., Elsheikh, A. H., Moustafa, E. B., Basha, M., and Showaib, E. A. (2021). Experimental investigation on laser cutting of PMMA sheets: Effects of process factors on kerf characteristics. *Journal of materials research and technology*, 11, 235-246. doi.org/10.1016/J.JMRT.2021.01.012
15. Masoud, F., Sapuan, S. M., Mohd Ariffin, M. K. A., Nukman, Y., and Bayraktar, E. (2020). Cutting processes of natural fiber-reinforced polymer composites. *Polymers*, 12(6), 1332. doi.org/10.3390/polym12061332
16. de Castro Monsorens, K. G., da Silva, A. O., Oliveira, S. D. S. A., Rodrigues, J. G. P., and Weber, R. P. (2019). Influence of ultraviolet radiation on polymethylmethacrylate (PMMA). *Journal of Materials Research and Technology*, 8(5), 3713-3718. doi.org/10.1016/J.JMRT.2019.06.023
17. Piana, G., Bella, F., Geobaldo, F., Meligrana, G., and Gerbaldi, C. (2019). PEO/LAGP hybrid solid polymer electrolytes for ambient temperature lithium batteries by solvent-free, "one pot" preparation. *Journal of Energy Storage*, 26, 100947. doi.org/10.1016/J.EST.2019.100947
18. Prakash, S., and Kumar, S. (2015). Fabrication of microchannels on transparent PMMA using CO₂ Laser (10.6 μm) for microfluidic applications: An experimental

investigation. *International Journal of Precision Engineering and Manufacturing*, 16, 361-366. doi.org/10.1007/s12541-015-0047-8

19. Sarikaya, M., and Yılmaz, V. (2018). Optimization and predictive modeling using S/N, RSM, RA and ANNs for micro-electrical discharge drilling of AISI 304 stainless steel. *Neural Computing and Applications*, 30, 1503-1517. doi.org/10.1007/s00521-016-2775-9
20. Son, S., and Lee, D. (2020). The effect of laser parameters on cutting metallic materials. *Materials*, 13(20), 4596. doi.org/10.3390/ma13204596
21. Vakili-Tahami, F., Adibeig, M. R., and Hassanifard, S. (2019). Optimizing creep lifetime of friction stir welded PMMA pipes subjected to combined loadings using rheological model. *Polymer Testing*, 79, 106049. doi.org/10.1016/j.polymertesting.2019.106049
22. Venkatesan, K., Ramanujam, R., & Kuppan, P. (2016). Parametric modeling and optimization of laser scanning parameters during laser assisted machining of Inconel 718. *Optics & Laser Technology*, 78, 10-18. doi.org/10.1016/j.optlastec.2015.09.021
23. Yüce, C. (2019). Paslanmaz çelik malzemelerin fiber lazer kesiminde proses parametrelerinin optimizasyonu. *Uludağ Üniversitesi Mühendislik Fakültesi Dergisi*, 24(2), 685-696. doi.org/10.17482/uumfd.514168